

An evaluation of Pt sulfite acid (PSA) as precursor for supported Pt catalysts

J.R. Regalbuto^{a,*}, O. Ansel^a, and J.T. Miller^b

^aDept. of Chem. Eng., U. of Illinois at Chicago, 810 S. Clinton Street, Chicago, IL, 60607 USA

^bBP Research Center, 150 W. Warrenville Rd., Naperville, IL, 60563 USA

As a catalyst precursor, platinum sulfite acid (PSA) is easy to use and not relatively expensive, and is a potentially attractive precursor for many types of supported catalysts. The ultimate usefulness for many catalyst applications will depend on the extent that Pt can be dispersed and sulfur eliminated. To our knowledge, there exists no detailed characterization in the catalysis literature of PSA and the nanoparticulate Pt phases derived from it during catalyst pretreatment. To this end a series of supports including alumina, silica, magnesia, niobia, titania, magnesia and carbon were contacted with PSA solutions and subsequently analyzed with extended x-ray absorption fine structure (EXAFS) and x-ray absorption near edge structure (XANES) analysis, and x-ray photoelectron spectroscopy (XPS) to characterize the Pt species formed upon impregnation, calcination, and reduction.

While all catalysts show retention of some S, reasonably small particle sizes with relatively little Pt-S can in some instances be produced using PSA. The amount of retained sulfur appears to decrease with decreasing surface acidity, although even the most acidic supports (niobia and silica) display some storage of S even while only Pt-O bands are observed after calcination or reoxidation. More sulfur was eliminated by high temperature calcinations followed by reduction in hydrogen, at the expense of increasing Pt particle size.

KEY WORDS: Catalyst synthesis; metal precursor; Pt Sulfite.

1. Introduction

As a catalyst precursor, platinum sulfite acid (PSA) is easy to use and not relatively expensive, and is a potentially attractive precursor for many types of supported catalysts. Commercially available in concentrated solutions (on the order of 10 wt% Pt), it is thought to be an anionic complex with two sulfurs and three acidic protons per Pt. The CAS structure of PSA is given in Figure 1 [1]. Historically, it has been a chloride-free intermediate in the synthesis of Pt/carbon black fuel cell electrocatalysts [2–5]. Pore filling (dry impregnation) of supports is perhaps the most attractive method of synthesis, potentially yielding small, well dispersed Pt nanoparticles from PSA is a single, simple preparation step. The ultimate usefulness for many catalyst applications will depend on the extent that Pt can be dispersed and sulfur eliminated. Sulfur poisoning has been cited in the case of electrodeposited PSA [4].

To this end a series of supports including alumina, silica, magnesia, niobia, titania, magnesia and carbon were contacted with PSA solutions and subsequently analyzed with extended x-ray absorption fine structure (EXAFS) and x-ray absorption near edge structure (XANES) analysis, and x-ray photoelectron spectroscopy (XPS) to characterize the Pt species formed upon

impregnation, calcination, and reduction.

2. Materials and Methods

A 10.4 wt% platinum sulfite acid solution was obtained from Heraeus and was diluted such that impregnation by pore filling (dry impregnation) into the various oxide and carbon supports yielded about 1.4 wt% Pt. This weight loading was chosen for its utility with EXAFS analysis. The various oxides employed are listed in Table 1, along with their PZCs which were measured by the “equilibrium pH at high loading” method [6]. PZC values ranged from very basic (magnesia) to very acidic (niobia). A range of titanias was used to determine the effect of surface impurities. Titania PZCs vary from 4 (Mirkat) to 6 (Sachtleben). The PZC of pure anatase titania is about 6 [7]. XPS analysis revealed that P25 contains a chloride impurity which lowers its PZC [8]. No chlorine or other anionic impurity was observed by XPS on Mirkat; the cause for its relatively low PZC is still unknown. All support materials were used in powder form to maximize the homogeneity of contact with the PSA solutions.

EXAFS and XANES measurements were performed at the Advanced Photon Source at Argonne National Laboratory with the MRCAT undulator beam-line equipped with a double-crystal Si (111) monochromator

* To whom correspondence should be addressed.
E-mail: jrr@uic.edu

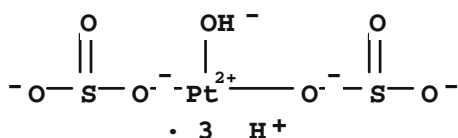


Figure 1. Chemical Abstracts-cited structure for PSA.

Table 1
PZCs and surface areas of supports

Support	PZC	SA (m ² /gm)
Nb ₂ O ₅	2.5	165
SiO ₂	4	220
Mirkat TiO ₂	4	165
P25 TiO ₂	4.5	50
Sachtleben TiO ₂	6	345
Al ₂ O ₃	8	277
Carbon black (Vulcan)	9	254
Carbon Black (BP 2000)	9	1500
MgO	13	14

with resolution of better than 4 eV at 11.5 keV (Pt L₃ edge). Spectra were taken in both the fluorescence and transmission modes using pressed powder samples. Phase-shift and backscattering amplitudes were obtained from various solid reference compounds. Details of the experimental and fitting procedures can be found elsewhere [9]. Results are shown as Fourier transformed spectra to emphasize the Pt-S, Pt-O and Pt-Pt (metal) content of samples.

The XPS measurements were made with an Kratos AXIS 165 instrument (monochromatic Al, hybrid mode) at UIC's RRC East facility. A resolution pass energy of 40 eV was used for core element analysis with 50 meV steps and 800 ms dwell time. Binding energies were corrected to adventitious carbon at 284.6 eV.

3. Results and Discussion

EXAFS results for concentrated PSA solutions (14,000 ppm Pt) at pH values of 1, which is the pH of the 14000 ppm solution diluted from the stock, and 6 and 13, attained by NaOH addition, are shown in figure 2. The structure of the complex varies relatively little with this large change in pH. Analysis of 1400 and 140 ppm solutions at the widely ranging pHs was similar. The complex appears to exist in solution with 2 Pt-S bonds and 2 Pt-O bonds, independent of pH and concentration. XANES revealed that the oxidation state of Pt is +2 at all pHs and concentrations. No precipitation was observed, thus the precursor is very robust and versatile in solution. The total number of ligands, 4, is consistent with Pt⁺² coordination complexes such as Pt(II) tetrachloride, [PtCl₄]⁻² and Pt (II) tetraammine, [(NH₃)₄Pt]⁺², and so the 3-coordinate structure postulated in Figure 1 [1] appears to be incorrect. The fourth

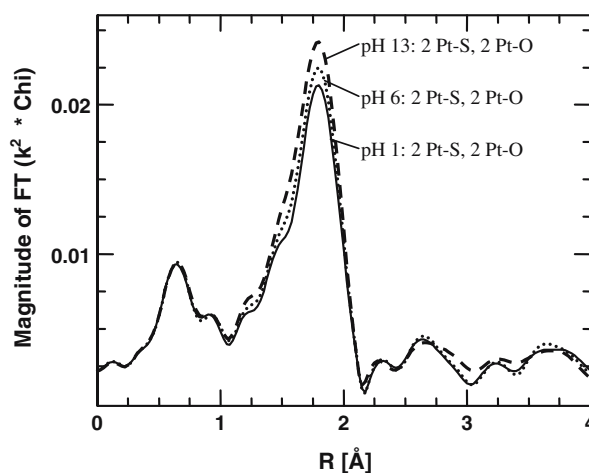


Figure 2. 2EXAFS spectra for 14,000 ppm PSA solutions as a function of pH.

ligand is perhaps water or OH⁻, coordinated through the oxygen.

EXAFS spectra for dried PSA adsorbed onto silica at pH 1 and 13 is shown in Figure 3; these two spectra are virtually unchanged from the solution spectra in Figure 2. The results are similar for every other oxide and carbon. These results are summarized in Table 2, along with values for the Debye Waller factor and E₀. XANES spectra are also unchanged; Pt exists in the +2 oxidation state. From the similarity of all adsorbed species, there does not appear to be any chemical interaction of the PSA complexes with the support surfaces.

The EXAFS results for the first coordination shell for all materials for all pretreatments studied are summarized in Table 3. Values of the DWF and E₀ are similar to those in Table 2 and are not listed. XANES estimations of the fractions of Pt⁺² and Pt⁰ will be described later in Table 4. Results will now be discussed in more detail with representative Fourier transform spectra.

Figure 4 illustrates various pretreatments of PSA adsorbed onto alumina. The dried precursor, which

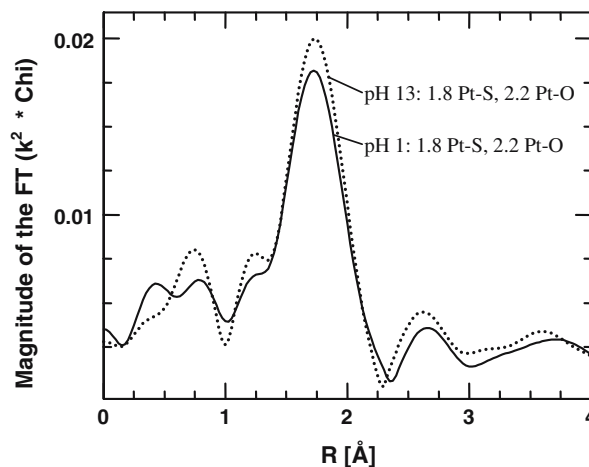


Figure 3. EXAFS spectra for PSA adsorbed onto silica at 1.4 wt% Pt, at different initial pHs.

Table 2
EXAFS analysis of impregnated, dried PSA on various supports

Catalyst	Treatment	Scatter	CN	R, Å	DWF ($\times 10^3$)	E0, eV
Nb ₂ O ₅	pH = 1	Pt-O	1.9	2.04	1.5	-4.0
		Pt-S	2.1	2.21	1.5	1.5
SiO ₂	pH = 1	Pt-O	2.2	2.04	2.0	-2.2
		Pt-S	1.8	2.21	2.0	-4.0
P25 TiO ₂	pH = 1	Pt-O	2.2	2.05	0.4	-4.4
		Pt-S	2.8	2.22	0.4	-0.8
Al ₂ O ₃	pH = 1	Pt-O	1.9	2.05	0.7	-0.6
		Pt-S	2.1	2.21	0.7	-4.6
Vulcan (Carbon)	pH = 1	Pt-O	2.1	2.05	1.0	-3.7
		Pt-S	1.9	2.20	1.0	-2.5
BP2000 (Carbon)	pH = 1	Pt-O	2.2	2.05	1.0	-3.0
		Pt-S	1.8	2.21	1.0	-2.1
MgO	pH = 1	Pt-O	2.0	2.05	0.6	-1.2
		Pt-S	2.0	2.21	0.6	-4.5

Table 3
EXAFS analysis of reduced PSA on various supports

Support SA (m ² /g)	bond	dried	Red 300	Red 500	Calc 300 Red 300	Calc 500 Red 300
Nb ₂ O ₅ 160	Pt-O	2	-	-	-	-
	Pt-S	2	2.3	.4	.4	.6
	Pt-Pt	-	-	6.2	7.7	6.0
SiO ₂ 220	Pt-O	2.2	-	-	-	-
	Pt-S	1.8	2.0	.8	1.0	.7
	Pt-Pt	-	3.5	8.4	7.4	8.7
TiO ₂ 165	Pt-O	2.0	-	-	n.a.	-
	Pt-S	2.2	3.1	1.2	n.a.	2.5
	Pt-Pt	-	-	2.7	n.a.	-
Al ₂ O ₃ 277	Pt-O	1.9	-	-	-	n.a.
	Pt-S	2.1	3.4	1.6	1.9	n.a.
	Pt-Pt	-	-	2.6	1.9	n.a.
V carbon 254	Pt-O	2.1	-	-	n.a.	n.a.
	Pt-S	1.9	3.1	1.5	n.a.	n.a.
	Pt-Pt	-	-	3.4	n.a.	n.a.
BP carbon 1500	Pt-O	2.2	-	-	n.a.	n.a.
	Pt-S	1.8	3.6	2.9	n.a.	n.a.
	Pt-Pt	-	-	-	n.a.	n.a.
MgO 14	Pt-O	2.0	-	-	n.a.	n.a.
	Pt-S	2.0	2.7	.9	n.a.	n.a.
	Pt-Pt	-	-	6.9	n.a.	n.a.

n.a.: not analyzed

once again contains two Pt-S and two Pt-O bonds, is seen in Figure 4a. When reduced at 300 °C in flowing hydrogen, only Pt-S bonds remain and no metallic Pt is created, as seen from the absence of Pt-Pt shells. Calcination of the dried precursor at 300 °C does lead to the breaking of the Pt-S bonds, as the precursor is converted to an oxide with about 6 Pt-O bonds. The removal of the Pt-S phase is only temporary, however. When the calcined sample is reduced, Pt-S bonds reform in addition to some metallic Pt (Figure 4b). Figure 4b also shows that a straight 500 °C reduction is also insufficient to remove the Pt-S phase.

The behavior of the mid-surface area titania (Mirkat) is illustrated in Figure 5. A straight 300 °C reduction

leads again only to Pt-S bonds, while a 500 °C reduction leads to more metallic Pt and a bit less Pt-S than over alumina. After 500 °C calcination, a 500 °C reduction was required to produce any Pt-Pt bonds, and the degree of reduction is a bit higher than the straight 500 °C reduction. Pt-S bonds still persist after the 500 °C calcination/500 °C reduction.

A comparison of all three titanias is seen in Table 3. While limited beam time prevented a complete comparison of pretreatments, some observations can be made. First, unlike the Mirkat shown in Figure 5, the low PZC, low surface area P25 sample yielded very large particles with mostly Pt-Pt bonds and some Pt-S even at 300 °C. The high surface area, high PZC Sachtleben sample retained more S and yielded the least amount of metallic Pt. The formation of poorly dispersed metallic Pt may be related to the relatively low surface area of the P25 material.

Metallic Pt forms to a greater extent over silica, as seen in Figure 6a. Already 3.5 Pt-Pt bonds arise after a 300 °C reduction, along with 2.0 Pt-S bonds. Calcination at 300 or 500 °C followed by reduction only serves to sinter the Pt-Pt phase and does not remove all Pt/S. In the most S-free sample (straight 500 °C reduction) there are on average 0.6 Pt-S bonds and 8.4 Pt-Pt bonds.

An attempt to remove sulfur from silica was made by a reduction-oxidation-reduction cycle (Figure 6b). From the 300 °C reduced sample (solid line) which contains about 2 Pt-S bonds and 3.5 Pt-Pt bonds, a 400 °C calcination once again removes the Pt-S bonds and an oxide phase is formed with 4.1 Pt-O bonds and 1.6 Pt-Pt bonds (dotted line). Upon re-reduction at 300 °C, Pt-S bonds form again with more Pt-Pt bonds than initially (dashed line). Again, some S is removed, but at the expense of sintering the metallic Pt.

The results for niobia are illustrated in Figure 7. Relatively smaller amounts of Pt-S are formed after reduction at 300 °C, with no Pt-Pt bonds. Calcination at 300 °C (Table 3) or 500 °C converts all Pt-S bonds to Pt-O. A 300 °C reduction of the 500 °C calcined sample leads to relatively small amounts of Pt-S, along with a moderately small Pt-Pt CN of 6. The smallest Pt-S CNs of any material studied (0.4 after 500 °C reduction) were seen over niobia (Table 3). Reduction – oxidation – reduction cycling was also conducted with niobia and was not any more successful in eliminating sulfur but again yielded a moderately small value of the Pt-Pt CN, 5.9.

A final comparison of catalyst supports with approximately the same surface area, including alumina, Mirkat titania, silica, and niobia, after an identical pretreatment (300 °C calcination followed by 300 °C reduction) is shown in figure 8. The amount of sulfur retained appears to decrease over this series, and can be correlated to their PZCs. The two carbons, also with high PZCs (Table 1) also retain much sulfur (Table 3).

The likely explanation for the trend in S retention is that the more basic surfaces have greater affinity for the

Table 4
Particle size estimates of reduced PSA on various supports

Sample	Pt-Pt CN	Fraction Pt ^{+2*}	Fraction Pt ⁰	Corrected Pt-Pt CN	Fraction Pt Surface Atoms	Estimated Particle Size, Å
Al red 300	-	1.0	-	-	-	No metallic Pt
Al cal 300 red 300	1.9	0.55	0.45	4.2	0.90	10
Al red 500	2.6	0.55	0.45	5.8	0.70	15
Si red 300	3.5	0.60	0.40	8.5	0.40	25
Si r300 o400 r300	5.2	0.40	0.60	8.6	0.40	25
Si cal 300 red 300	7.4	0.30	0.70	10.6	0.15	60
Si cal 500 red 300	8.7	0.20	0.80	10.9	0.15	75
Si red 500	8.4	0.20	0.80	10.5	0.15	60
Mg red 300	-	1.0	-	-	-	No metallic Pt
Mg red 500	6.9	0.30	0.70	9.9	0.25	40
Nb red 500	6.2	0.15	0.85	7.3	0.55	20
Ti* red 300	6.0	0.35	0.65	9.2	0.35	30
Ti* cal 500 red 300	11.3	0.25	0.75	15	<0.1	>100
V carbon red 300	-	1.0	-	-	-	No metallic Pt
V carbon red 500	3.4	0.50	0.50	6.8	0.60	20
BP red 300	-	1.0	-	-	-	No metallic Pt
BP red 500	-	1.0	-	-	-	No metallic Pt

*Mirkat TiO₂

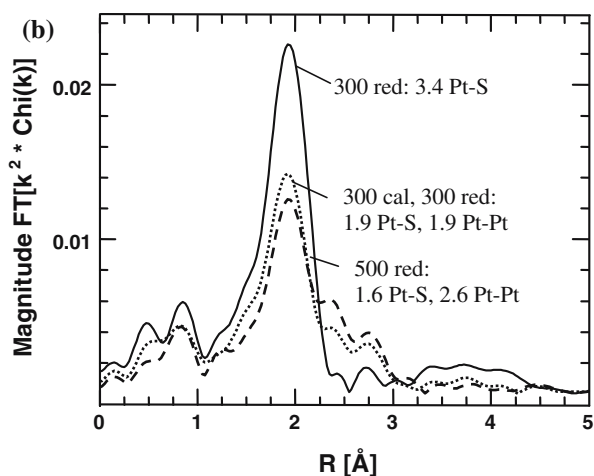
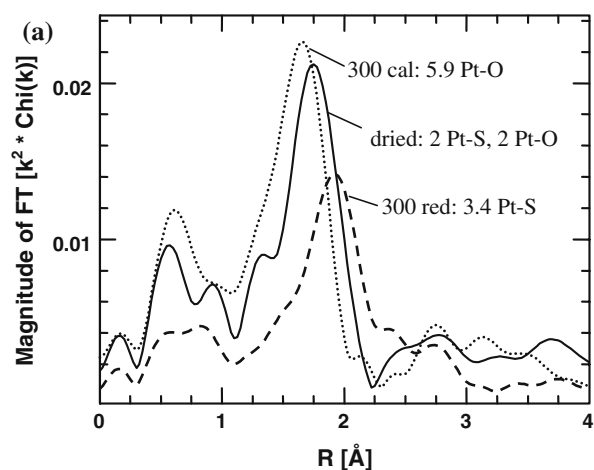


Figure 4. EXAFS spectra for PSA/alumina (1.4 wt% Pt) after various pretreatments, a) 300°C calcination or reduction, b) calcination followed by reduction, and 500°C reduction.

acidic sulfur-containing species such as sulfate which form during pretreatment. Even though calcination of a dried precursor or oxidation of a reduced one (Table 3) destroys all Pt-S bonds, the sulfur-containing species would be more readily stored on the more basic support surfaces. Silica and niobia supported PSA also have some mechanism for S storage, however, since small amounts of S reappear. The sulfur is perhaps associated with the Pt phase as Pt-O-S linkages in those calcined materials.

The trend of sulfur retention with PZC is also manifested in XPS data. In Figure 9, the percent decrease in atomic percent S is plotted for all supports studied. The supports are arranged from the lowest PZC on the left, to the highest PZC on the right. The general trend is the

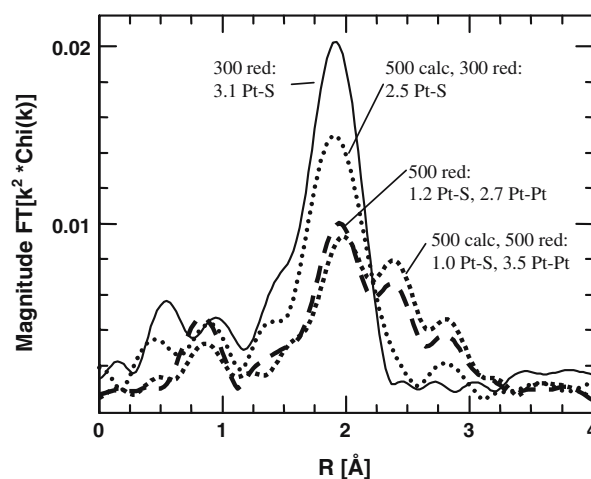


Figure 5. EXAFS spectra for PSA/ Mirkat titania (1.4 wt% Pt) after various pretreatments.

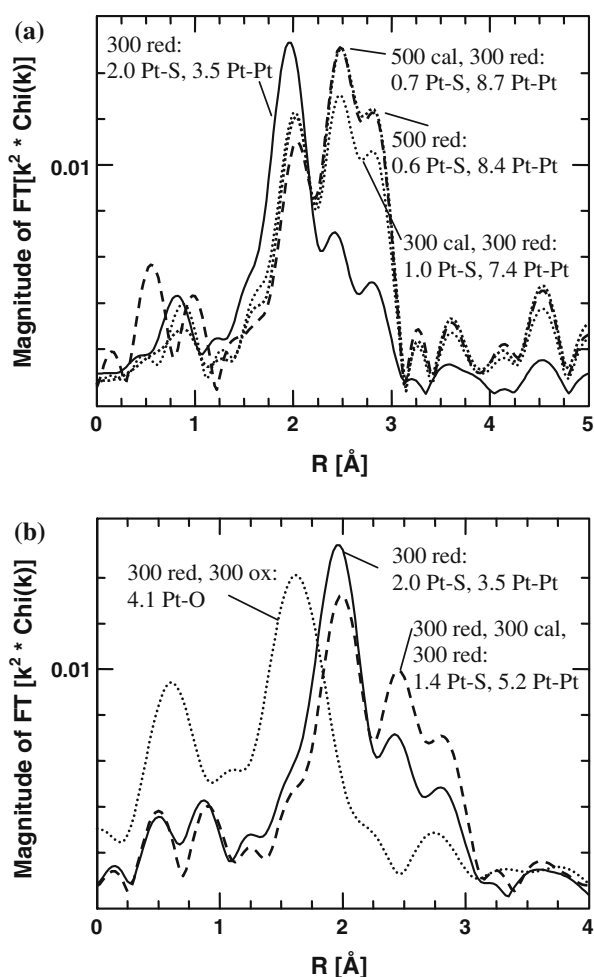


Figure 6. EXAFS spectra for PSA/silica (1.4 wt% Pt) after various pretreatments, a) reduction or reduction following calcination, b) oxidation after reduction.

lower the PZC, the greater the fraction of sulfur removed. For the magnesia sample, the amount of sulfur actually increases after reduction (and is represented by a “negative” decrease). Since XPS is sensitive to only the top few atomic layers of the material, the increase in the S signal indicates that the sulfur species spread over the surface during reduction.

Another pertinent measurement from XPS is the S/Pt ratio. This ratio is influenced by the dispersion of both the sulfur and the Pt phases. In Figure 10 of particular note is that the S/Pt ratio decreases after reduction for the oxides with the lower PZCs, while the ratio increases for the supports with PZCs of 6 or greater. This trend can be explained by two contributing factors: as the PZC increases, S retention increases and the S signal becomes relatively larger, and second, as the PZC increases, electrostatic interaction with the anionic PSA complex should increase, leading to more highly dispersed Pt and a higher Pt XPS signal.

The valence of Pt, as determined from XPS by deconvolution of the Pt 4f envelope, was quite consistent

with values determined from XANES (Table 4). The dried PSA precursor is confirmed by XPS to be Pt⁺² over all supports. Fractions of Pt⁺² and Pt⁰ in the reduced samples were within 10 % of the values as determined from XANES (Table 4), with the exception of the 300 °C reduced SiO₂ sample. For this sample the fractions of Pt⁺² and Pt⁰ were determined to be 60 and 40% from EXAFS, but 30 and 70% from XPS.

A final consideration can be made concerning the size of Pt containing particles. While estimation of Pt particle sizes can be made straightforwardly for pure Pt metal particles, from a correlation of Pt-Pt coordination numbers with Pt dispersion measured by H₂ chemisorption [10], estimating the size of particles containing a fraction of Pt-S is more tenuous. Nevertheless, an estimate has been attempted and can at least serve to indicate the general trends in the size of Pt-containing particles which result from the PSA precursor.

The data from which estimates were made is given in Table 4. It was assumed that the Pt on Al, V and BP carbons reduced at 300 °C was 100% Pt⁺² (i.e., PtS) since these did not have a Pt-Pt in the EXAFS and the

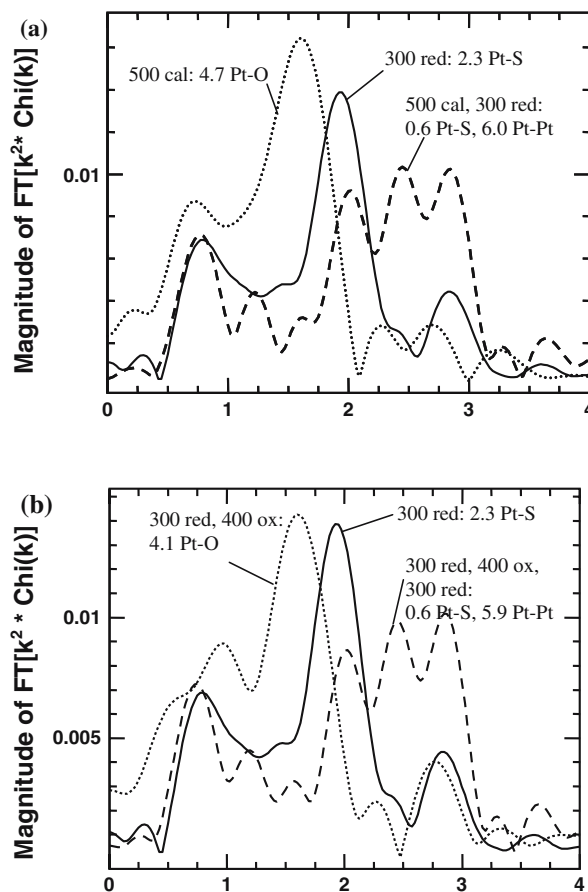


Figure 7. EXAFS spectra for PSA/niobia (1.4 wt% Pt) after various pretreatments, a) reduction or reduction following calcination, b) oxidation after reduction.

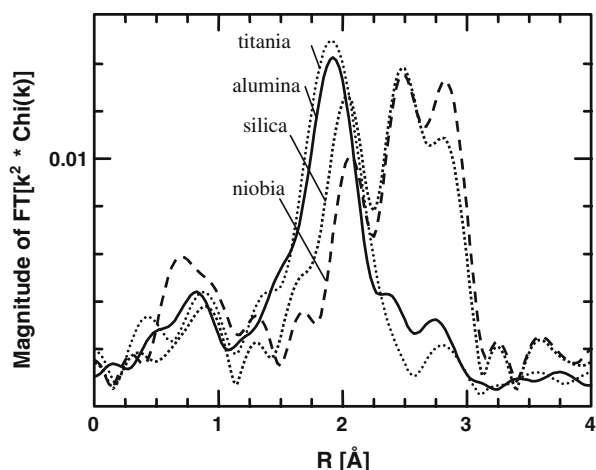


Figure 8. EXAFS spectra for PSA (1.4 wt% Pt) on various supports, after 300 °C calcination and 300 °C reduction (Mirkat titania: 500 °C calcination and 300 °C reduction).

XANES was similar to Pt^{+2} . The Pt-S average CN for these three catalysts was 3.4. For all other catalysts reduced at 300 °C, the fraction of Pt^{+2} was taken as the Pt-S CN/3.4. The remaining Pt is then metallic. The fitted CN was then divided by the fraction of Pt^0 to get the corrected Pt-Pt CN. From that, the fraction of surface Pt atoms in the metallic particle could be estimated (this fraction is not properly termed “dispersion” since they have S on them) using the correlation of H_2 chemisorption and Pt-Pt CN. Assuming spherical geometry, size can be estimated as $1/\text{dispersion} \times 10 \text{ \AA}$. For catalyst reduced at 500 °C, the same approach was taken. However, 2.9 Pt-S, which is the value for BP carbon reduced at 500 °C, was used as 100% Pt^{+2} .

The fraction of surface atoms and particle sizes should be viewed as very approximate and might be used to classify the particles as small, medium and large. There is a significant fraction (25–50%) of Pt^{+2} , i.e., a high fraction of Pt is bonded to S, in most catalysts. For example, while silica yields small particles, they contain a high fraction of sulfur. For most catalysts the fraction of surface Pt atoms is similar to the fraction of Pt^{+2} , i.e., atoms with S. Thus, there is not a lot of exposed, reduced Pt. In practice, many (reduced) catalysts are completely poisoned when there is 1 S for every 3 surface Pt atoms. The best support appears to be Nb_2O_5 , over which the particles are small-medium in size, but have a much smaller fraction of Pt-S, about 10–15%.

4. Conclusions

While all catalysts show retention of some S, reasonably small particle sizes with relatively little Pt-S can in some instances be produced using PSA. The amount of retained sulfur appears to decrease with decreasing surface acidity, although even the most acidic supports (niobia and silica) display some storage of S even while only Pt-O bands are observed after calcination or reoxidation. More sulfur was eliminated by high temperature calcinations followed by reduction in hydrogen, at the expense of increasing Pt particle size.

While this synthesis approach would not appear to be very good for sulfur-poisoned catalysts used for example in reforming or other reduction reactions, it maybe suitable for those applications such as automobile

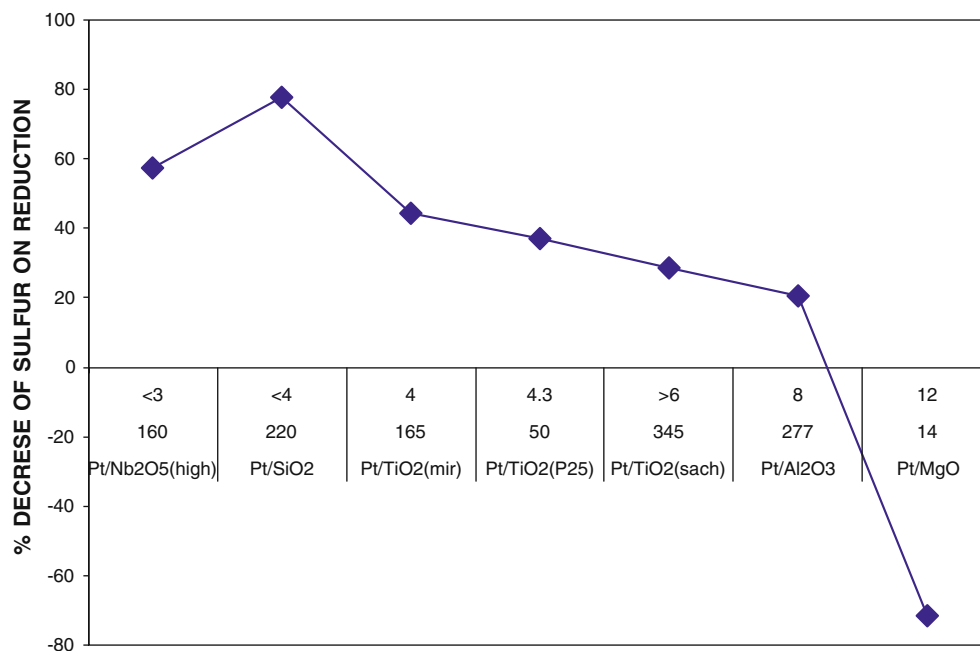


Figure 9. XPS analysis of percent S removal after reduction, on various supports.

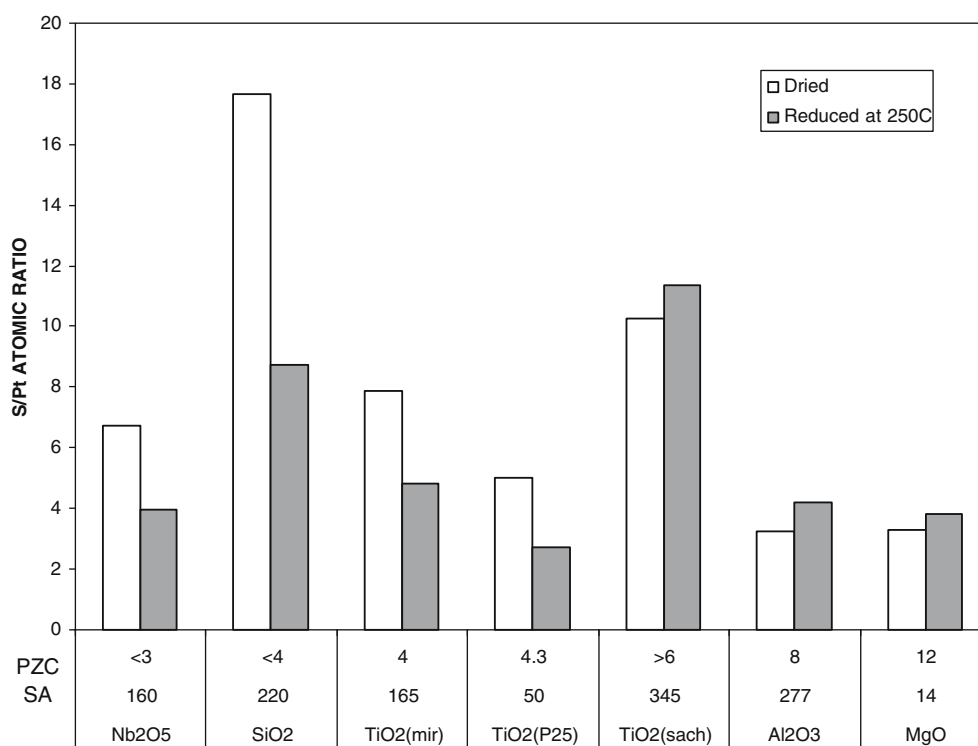


Figure 10. XPS analysis of S/Pt atomic ratios, on various supports, before and after reduction.

exhaust catalysts which employ sulfur getters such as Ni that may serve to keep the Pt surface free of sulfur.

Acknowledgments

JRR gratefully acknowledges the support of the Companhia Brasileira de Metalurgia e Mineração (CBMM) and the National Science Foundation (NSF CTS-0243210). Use of the Advanced Photon Source was supported by the U. S. Department of Energy, Office of Science, Office of Basic Energy Sciences, under Contract No. W-31-109-Eng-38. Work performed at MRCAT is supported, in part by funding from the Department of Energy under grant number DE-FG02-04ER 46106. The submitted manuscript has been created by the University of Chicago as Operator of Argonne National Laboratory under Contract No. W-31-109-Eng-38 with the U.S. Department of Energy. The U.S. Government retains for itself, and others acting on its behalf, a paid-up, nonexclusive, irrevocable worldwide

license in said article to reproduce, prepare derivative works, distribute copies to the public, and perform publicly and display publicly, by or on behalf of the Government.

References

- [1] CAS registry number 61420-92-6.
- [2] M. Watanabe et al., J. Electroanal. Chem. 229 (1987) 395.
- [3] Petrow, H.G., and Allen, R.J., U.S. Patent 4,044,193.
- [4] S.D. Thompson, L.R. Jordan, A.K. Shukla and M Forsyth, J. Electroanal. Chem. 515 (2001) 61.
- [5] T. Milusheva, I. Nikolov, V. Naidenov and T Vitanov, Bulg. Chem. Comm. 36 (2004) 117.
- [6] J.-H. Park and J.R. Regalbuto, J. of Coll. Interf. Sci. 175 (1995) 239.
- [7] G.A Parks, Chem. Rev. 65 (1965) 177.
- [8] W. Spieker, J. Regalbuto, D. Rende, M. Bricker and Q Chen, Stud. Surf. Sci. Catal. 130 (2000) 203.
- [9] W.A. Spieker, J. Liu, X. Hao, J.T. Miller, A.J. Kropf and J.R. Regalbuto, Appl. Catal. A: Gen. 243 (2003) 53.
- [10] J. T. Miller, et al., J. Catal. 240 (2006) 222.